

RESEARCH

Open Access



Molecular characterization and complexity of the immunoglobulin repertoire in the silver-black fox (*Vulpes vulpes*)

Xiaohua Yi^{1†}, Yanbo Qiu^{2†}, Puhang Xie², Shuhui Wang^{1*} and Xiuzhu Sun^{2*}

Abstract

Immunoglobulins, a class of globulins with antibody properties, play a crucial role in the body's defense against pathogens. In this study, we analyzed the gene loci structure of Silver-black fox using a comparative genomics approach. The mechanisms of expression diversity and its preferences were investigated through Next-generation sequencing (NGS). The results revealed 32 potentially functional VH genes, 9 Vk genes, 17 Vλ genes, 9 DH genes, 3 JH genes, 6 Jk genes, and 11 Jλ genes, located on different scaffolds. Subsequently, 5'RACE and PE300 bipartite sequencing were used to obtain the reads of the expressed antibody repertoire of Silver-black foxes gene rearrangement events. The analysis indicated a strong preference in the use of V genes, DH genes and J genes by Silver-black fox. The main ways of expression diversity were V(D)J recombination and somatic hypermutation (SHM). The hypermutated region of SHM was not only concentrated in the CDR region but also had higher mutation rate in the FR region. The main types of SHM were G > A, C > T, T > C, and A > G. The findings of this study could serve as a theoretical foundation for a deeper understanding of Silver-black fox immunoglobulins, which is significant for enriching knowledge in immunogenetics and providing theoretical support for future studies on vaccine design for the Silver-black fox.

Keywords Silver-black fox, Immunoglobulin, IgH, Igk, Igλ

Introduction

Immunoglobulin (Ig) functions as a key molecular marker for adaptive immunity in jawed vertebrates, playing a pivotal role in the immune defense mechanisms of these species, including humans [1]. The classical Ig monomer molecule is a symmetric structure consisting of two identical heavy chains (H chains) of high relative molecular mass and two identical light chains (L chains) of low relative molecular mass, which are connected by disulfide bonds, giving the appearance of a “Y” structure [2–5]. The H and L chains are composed of multiple structural domains, each containing approximately 100–110 amino acid residues. The light chain typically consists of two structural domains, each around 25 kDa, while the heavy chain generally comprises 4–5 structural domains

[†]Xiaohua Yi and Yanbo Qiu have contributed equally to this work.

*Correspondence:

Shuhui Wang
wangshuhui252@163.com
Xiuzhu Sun
sunxiuzhu@nwfau.edu.cn

¹College of Animal Science and Technology, Northwest A&F University, Yangling 712100, China

²College of Grassland Agriculture, Northwest A&F University, Yangling 712100, China



with molecular weights ranging from 50–75 kDa. The variable regions originate from a series of complex gene rearrangement events. Each variable domain can be divided into four relatively constant sequence regions, commonly referred to as framework regions (FRs) [6]. Additionally, there are three sequence regions prone to mutations, known as complementarity-determining regions (CDRs). The variable region of the Ig heavy chain is coded by three distinct gene segments, namely variable (V), diversity (D), and joining (J) genes, while the variable region of the light chain is coded by two gene segments: V and J [7]. The V gene segment corresponds to the CDR1 and CDR2 of the complementary determining regions; the D gene segment primarily encodes the central portion of CDR3 in the heavy chain variable region; and the J gene is located at the 3' end of the DH gene, corresponding to the remaining part of the variable region CDR3 and FR4 [8]. The carboxyl-terminal (C-terminal) regions of the H and L chains are referred to as the constant region (C region), which is a crucial part for the Ig molecule to exert its effector functions. Among them, the constant region of the heavy chain is designated as CH, and that of the light chain as CL. According to the differences in the physicochemical properties and antigenic epitopes of CH, most mammalian heavy chains can be classified into five types, namely μ , δ , γ , ϵ , and α , and the corresponding Igs are IgM, IgD, IgG, IgE, and IgA, respectively [9]. Moreover, Igs of the same class across different species can differentiate into distinct subclasses based on subtle structural differences in the CH region, such as the number of disulfide bonds, spatial distribution, and antigen specificity [10, 11]. The heavy chain comprises several constant regions, which are designated as CH1, CH2, CH3, and so on [12]. The heavy chain of the Ig molecule contains a hinge region between the CH1 and CH2 regions, which enhances its spatial and structural flexibility. The amino acid sequences in the constant region are relatively conserved and primarily responsible for binding to specific receptors, which in turn regulate the activity of various immune cells and mediate diverse immune responses [13].

It has been shown that the germline antibody repertoire and the (auto) antigen recognition of an individual is determined by recombination between segments of the Ig gene [14]. It has been demonstrated that there are four primary mechanisms for generating Ig diversity: V(D)J recombination, gene conversion (GCV), somatic hypermutation (SHM), and class switch recombination (CSR) [15–17]. With the exception of CSR, all of these mechanisms contribute to the diversity of variable regions [18–22]. The V(D)J recombination process is initiated by the recombinase encoded by the recombination activating genes (RAG1–RAG2) at specific recombination signal sequences (RSS), resulting in double-strand breaks

(DSBs). RSS typically consist of a highly conserved heptamer (consensus sequence 5'-CACAGTG-3') and a conserved nonamer sequence (consensus sequence 5'-ACAAAACC-3'), separated by a less conserved spacer sequence of 12 or 23 nucleotides. During V(D)J recombination, the addition of nontemplated nucleotides (N-nucleotides) at coding joints and signal joints is almost mediated by terminal deoxynucleotidyl transferase (TdT) [23, 24]. TdT is an enzyme that plays a crucial role during lymphocyte development, where it adds nucleotide residues in a template-independent manner at the ends of DNA breaks, thereby increasing the diversity of antibodies and T cell receptors [25, 26]. The activity of TdT is essential for the generation of a diverse immune receptor repertoire during V(D)J recombination [27]. The formation of palindromic nucleotides (P-nucleotides) occurs due to asymmetric cleavage and filling of the DNA hairpin structure during the repair process, resulting in symmetric nucleotide sequences at the junctions [28], specifically when the RAG1 and RAG2 enzyme complex opens the DNA hairpin structure. The addition of N and P nucleotides contributes to the diversification of Ig gene expression to some extent, enabling the organism to effectively recognize and respond to various pathogenic challenges.

Following V(D)J recombination, B cells undergo two subsequent genetic modifications: SHM and CSR. These alterations, which occur mainly in the germinal center, aim to enhance the affinity and modulate the biological properties of Igs with specificity towards the antigen. Notably, in some species (e.g., chickens), the Ig repertoire is limited by a finite number of potential functional V and J genes, making the generation of Ig diversity through V(D)J recombination highly restricted. However, their Igs can compensate for this limitation by utilizing GCV as an alternative mechanism [29]. The molecular mechanisms underlying SHM, CSR, and GCV exhibit numerous parallels and involve activation induced enzymatic pathways. Among them, activation-induced cytidine deaminase (AID) is considered to be a key factor indispensable for the processes of SHM and CSR [30]. Organisms utilize the aforementioned mechanisms to enhance the diversity of the antibody repertoire. Based on current knowledge, the human antibody repertoire consists of approximately 3×10^{15} Igs, a number significantly surpassing the count of human germline genes [31–33]. This abundance serves as the foundation for human defense against the onslaught of myriad antigenic challenges.

Previous research has extensively explored the Ig locus in various mammals, including yaks [34], goats [35, 36], horses [37], cows [38], and others. Notably, the domestic dog (*Canis lupus familiaris*), which belongs to the family of Canidae, was found to have a total of 80 VH gene fragments, 6 DH gene fragments and 3 JH gene fragments

identified in its IGH loci. Based on their nucleotide identity, the 80 canine VH genes were classified into three families. The first family consisted of 76 sequences, whereas the other four VH genes, VH51, VH64, and VH66, had greater than 80% nucleotide similarity and were classified as the second canine family. For VH80, its nucleotide identity was less than 70% in all other sequences, indicating that it belongs to a single member family [39]. A recent study in dogs identified nine J-C pairs, 162 IGLV, 19 IGKV, 5 IGKJ, and one IGKC gene in the IGL. In addition, three novel IGHJ genes were also identified [40].

The Silver-black fox (*Vulpes vulpes*), like domestic dogs, belongs to the family Canidae of the order Carnivora within the class Mammalia. It is a recessive mutant variant of the wild red fox that occurs under natural conditions. Characterized by a relatively large and compact body, well-proportioned physique, unique fur coloration, and high-quality pelt, the Silver-black fox is a valuable fur-bearing species [41]. Ig serves as key mediators of humoral immune responses, and elucidating their genetic structure is crucial for understanding immune regulatory mechanisms and advancing disease-resistance breeding strategies. However, research on the germline Ig genes and their diversified expression in the Silver-black fox remains in its early stages. This study aims to comprehensively analyze the loci structure and expression diversity of Ig genes in the Silver-black fox, providing a theoretical foundation for the development of disease-resistant breeding programs and contributing to the establishment of a scientific health management system for farmed populations.

Materials and methods

Animals, RNA isolations

The experiment utilized three Silver-black foxes (8 months old) obtained from the Jiao Agricultural Feeding Farm fox breeding facility (Changli, Hebei, China). These foxes were inoculated with the same doses of the water ferret parvovirus enteritis inactivated vaccine (MEVB strain) and the ferret canine distemper live vaccine (CDV3-CL strain), and were maintained under identical husbandry conditions. In order to minimize the animal's physical and psychological suffering, these Silver-black foxes were first anesthetized with halothane (5% concentration) and bled to death while unconscious. Spleen samples were collected from all three foxes, preserved in liquid nitrogen and stored at -80°C . Total RNA from the spleen tissues was extracted using the Trizol method (Takara, Dalian). The RNA quality was assessed, and the RNA concentration was measured using Nanodrop1000 (Thermo Fisher Scientific, USA). The total RNA samples were stored in an ultra-low temperature freezer at -80°C .

Analysis of the immunoglobulin gene loci in silver-black fox

This study was based on the genome data of the Silver-black fox (GCF_003160815.1) publicly available in the NCBI database (<http://www.ncbi.nlm.nih.gov>), as well as sequences from other species including humans, mice, pigs, cattle, and dogs, encompassing VH, DH, JH, V λ , J λ , V κ , J κ genes, and constant region genes μ , δ , α , γ , ϵ , λ , and κ . Initially, the positions of VH, DH, JH, V λ , J λ , V κ , J κ , μ , δ , α , γ , ϵ , λ , and κ genes in the Silver-black fox genome were determined through BLAST analysis. Subsequently, FUZZNUC website (www-archbac.u-psud.fr/genomics/patternSearch.html) was utilized to retrieve RSS sequences conforming to the 12/23 rule, while considering 5 base mismatches, followed by the identification of potential D genes and J genes. According to the IMGT rules, all retrieved V genes were categorized into potential functional genes, pseudogenes, and open reading frames [42]. Finally, a physical map of the IgH, Ig λ , and Ig κ gene positions was constructed based on the identified gene locations.

Phylogenetic analysis

The nucleotide similarity of the searched Silver-black fox VH gene sequences was analyzed using DNAMAN 6.0. Sequences with more than 75% identity were classified into the same gene family, those with less than 70% identity were classified into different gene families, and those with 70–75% identity were categorized based on additional factors, such as phylogenetic analysis, functional motifs. Furthermore, the homology of the FR1~FR3 region of the Silver-black fox VH gene was analyzed using MEGA11.0 software, comparing it with reference sequences from human, mouse, cow, sheep, horse, frog, chicken, African clawed frog, zebrafish and nurse shark. The reference names and numbering of the V and ORF genes for the species involved in the construction of the phylogenetic tree, excluding the Silver-black fox, are provided in Supplementary File A.

Silver-black Fox 5'-RACE-ready cDNA synthesis and rapid amplification of cDNA ends

The 5'-RACE-Ready cDNA synthesis was performed using the SMARTer™ RACE 5'/3' Kit (Takara Dalian). For target gene amplification, the Universal Primer Mix (UPM: 5'-AAGCAGTGGTATCAACGCAGAGT-3') provided in the kit served as the forward primer. Reverse gene-specific primers (GSP) were designed as follows: the heavy chain primer (GSP-H: 5'-GACAGGGAGTTCTCA CAGGTGAT-3') targeted the C μ domain, while the light chain primers (GSP- λ : 5'-GAGGGCGGGAAGAGAGAG TGACCGA-3'; GSP- κ : 5'-TAGACGGCTGGCTGGGCA TCATT-3') were derived from the CL and C κ domains, respectively. PCR amplification was conducted using the

high-fidelity DNA polymerase included in the SMART™ 5' RACE Kit (Takara, Dalian). The amplification products were separated by electrophoresis on 1.5% agarose gels for 30 min and then validated by Sanger sequencing. All reactions were performed in triplicate to ensure technical reproducibility.

DNA library Preparation and illumina miseq PE300 platform sequencing

The specific amplification products were used to construct libraries, and qualified libraries were subjected to paired-end 300 bp (PE300) sequencing on the Illumina MiSeq PE300 platform (Sangon Biotech, China). After high-throughput sequencing data were generated, the first step was to perform data quality control. The main process is that the Cutadapt software (v1.2.1) was used with default parameters to remove adapter sequences. The Pear software (v0.9.6) was then employed to merge forward and reverse reads of the same sequence into a single chain. Pinseq-lite software (v0.19.5) was utilized to remove low-quality bases and sequences. Chimera sequences were eliminated using Usearch software (v11.0.667) in de novo mode. Subsequently, target sequences were identified based on specific forward and reverse primer sequences.

Bioinformatics analysis

The IMGT (ImMunoGeneTics) database classifies Ig genes into different subgroups based on their function and structure. According to the IG nomenclature rules, sequencing-derived valid sequences (excluding excessively short or truncated sequences) are assigned to specific subgroups. The “NGS High-Throughput Analysis” function (<https://www.imgt.org/HighV-QUEST/>) in IMGT was utilized for the analysis of these valid sequences. This study conducted an in-depth investigation of V(D)J recombination, junctional diversity, and SHM in the Silver-black fox. For V(D)J recombination, the V, D, and J genes were first classified into subgroups, followed by an analysis of subgroup usage frequency and V(D)J combination patterns. In the analysis of junctional diversity, we examined the insertion of N and P nucleotides, the deletion of 3'V-Region and 5'J-Region genes, and the characteristics of the CDR3 sequences. The SHM analysis focused on the types of nucleotide mutations and their occurrence sites. For data visualization, this study primarily employed the Lianchuan Bio Cloud Platform (<https://www.omicstudio.cn/tool>) and GraphPad Prism 9.5.

Results

Structure of the genomic organization and phylogenetic analysis of silver-black Fox IgH

We found that Silver-black fox VH genes were distributed over 32 scaffolds, including 32 potentially functional

VH genes and 24 pseudogenes, with the pseudogenes included some incomplete gene fragments (Fig. 1A). Specifically, all potentially functional genes had a complete V region structure, as well as the conserved amino acid sequences 23-Cys, 41-Trp, and 104-Cys. In addition, we identified 3 potentially functional JH genes, 9 potentially functional DH genes, and structurally complete μ , δ , γ , ϵ , and α genes, which were located on the same scaffold and they were all arranged in reverse order, which may be caused by the reverse placement of the scaffold during genome assembly (Fig. 1A). All three JH genes have the conserved amino acid structure of WGXXG and end with the conserved amino acid structure of TVSS. Subsequently, we classified all VH genes into families based on nucleotide identity and found that all VH genes could be classified into three families and potentially functional VH genes were distributed in all four family species (Fig. 1B). Further, we performed an evolutionary analysis of the relationship between potentially functional VH genes and VH genes of representative mammals, and found that Silver-black fox VH genes were more closely related to humans and dogs (Fig. 1C).

Analysis of the use of the VH, DH, and JH genes in the silver-black Fox

To analyze the VDJ gene usage after Silver-black fox recombination, we named all valid reads obtained by sequencing according to IMGT-subgroup, and then analyzed the gene usage of each type, as shown in Fig. 2. Frequency analysis of VH gene usage revealed that the three samples performed consistently, with IGHV3 being used more than 96.35% and only about 1% using IGHV1 (Fig. 2A). Similarly, we analyzed the frequency of use of DH and JH genes, with the most used DH gene being IGHD2 (>27%) (Fig. 2B) and the most used JH gene being IGHJ4 (>68%) (Fig. 2C). In terms of the number of VDJ genes used, the expression trend was also consistent across the three samples (Fig. 2D-F).

Analysis of VDJ recombination diversity and junction diversity in the silver-black Fox IgH

As shown in Figure S1A, only IGHV3 was predominantly expressed by the VH gene of Silver-black fox IgH, whereas five DH and JH genes were expressed. The overall usage of the three samples tended to be consistent, but there were some differences in the combinations. Specifically, the most used combinations in Sample 1 were IGHV3-IGHD2-IGHJ4 (25.2%), IGHV3-IGHD4-IGHJ4 (22.1%) and IGHV3-IGHD3-IGHJ4 (10.2%), the more used combination in Sample 2 were IGHV3-IGHD4-IGHJ4 (26.2%), IGHV3-IGHD2-IGHJ4 (22.8%) and IGHV3-IGHD1-IGHJ4 (9.7%), and the most used combinations in Sample 3 were IGHV3-IGHD2-IGHJ4 (20.5%), IGHV3-IGHD1-IGHJ4 (17.9%) and

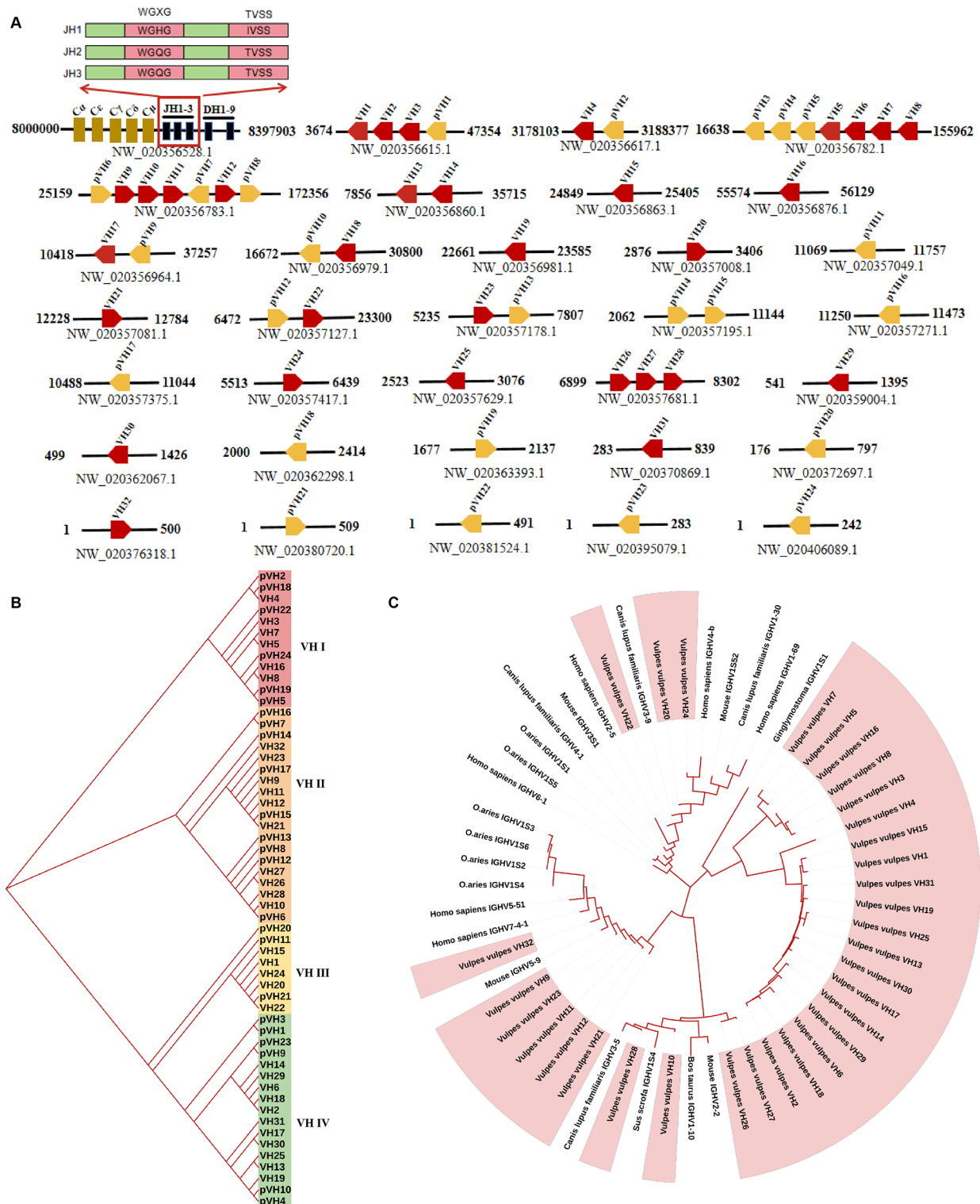


Fig. 1 Structure of the genomic organization and phylogenetic analysis of Silver-black Fox IgH. **A:** IgH gene loci structure in Silver Fox; **B:** Phylogenetic tree of VH gene in Silver Fox; **C:** Phylogenetic tree of Silver Fox and representative vertebrate VH. Note: Fig. 1A: The 32 scaffolds of the IgH gene are plotted along with the corresponding ID sequence numbers. The start and end positions of each scaffold are labeled in the figure. Red arrows represent functional VH genes, yellow arrows represent pseudogenes, and the head of each arrow indicates the orientation of the gene in the genome. The squares in scaffold 8,000,000–8,397,903 contain potentially functional JH and DH genes, and the JH conserved amino acid structure is shown above them

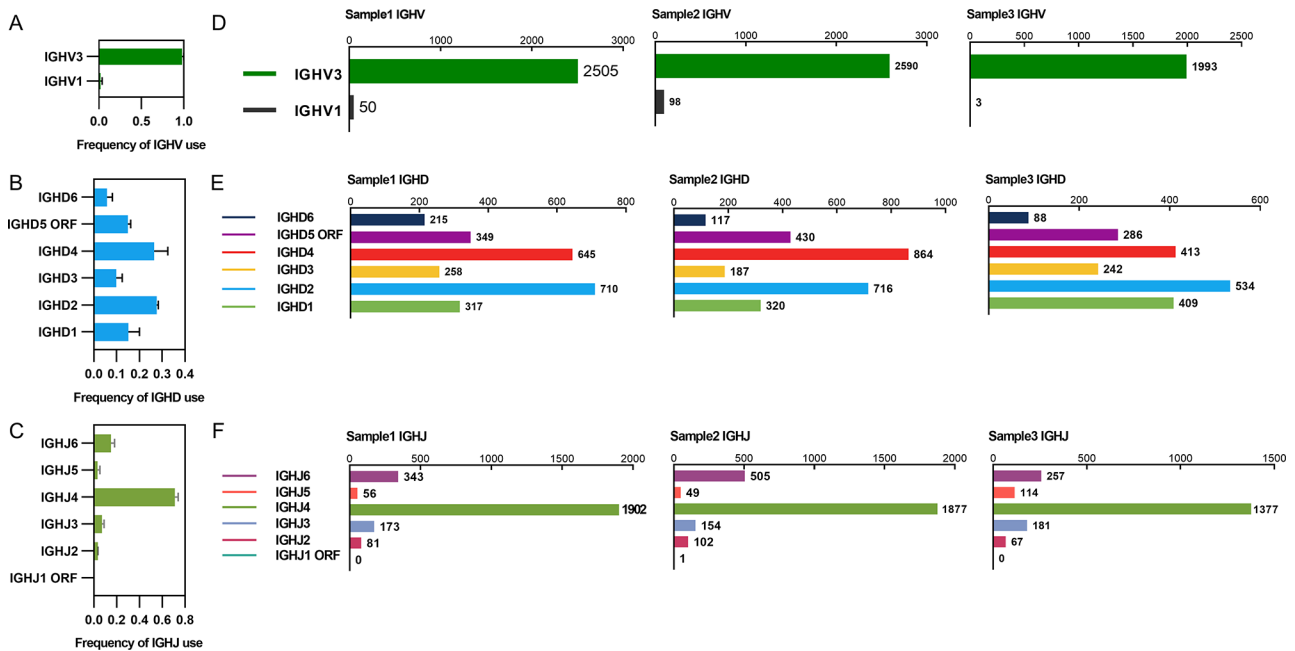


Fig. 2 Analysis of Silver-black Fox VH, DH and JH usage. **A&D:** Expression of the Silver-black Fox VH; **B&E:** Expression of the Silver-black Fox DH; **C&F:** Expression of the Silver-black Fox JH. Note: The X-axis numbers in Figure D-F represent read readings

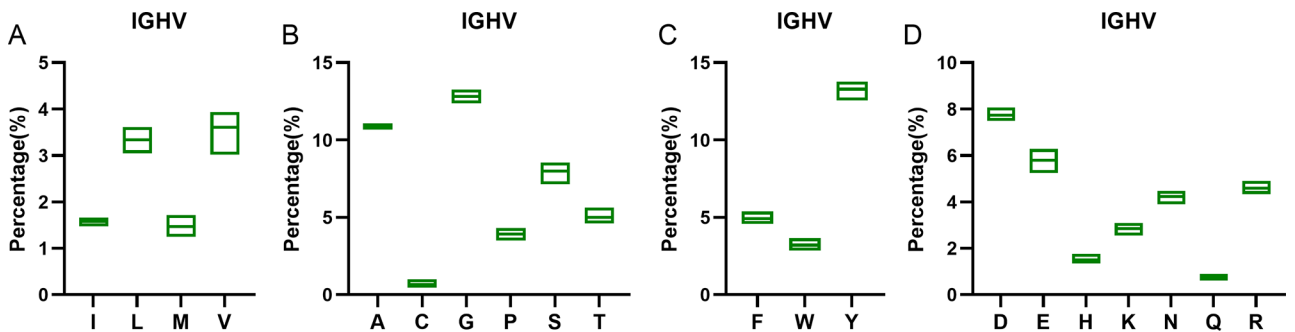


Fig. 3 Frequency of various amino acids used in CDR3H of Silver-black Fox. **A:** Frequency of hydrophobic amino acids in CDR3H of Silver-black Fox; **B:** Frequency of small molecular functional group amino acids in CDR3H of Silver-black Fox; **C:** Frequency of use of aromatic amino acids in CDR3H of Silver-black Fox; **D:** Frequency of use of charged amino acids in CDR3H of Silver-black Fox

IGHV3-IGHD4-IGHJ4 (17.3%). In addition, we analyzed the length distribution of the CDR3 region and the insertion of N/P nucleotides. As shown in Figure S1B, random deletions of VH genes were mainly distributed in 0–6 bp, with the majority of 0 bp and 6 bp, indicating that most random deletions of VH genes do not produce shifted-code mutations. Random deletions of JH genes were distributed in 0–11 bp, with the majority of 2 bp and 5 bp, which may lead to shifted-code mutations of recombinant sequences after deletion (Figure S1C). Insertions of N/P nucleotides were mainly distributed at 0 bp, indicating that the insertion of NP nucleotides contributed less to the length diversity of CDR3 (Figure S1G-H). Finally, we analyzed the lengths of the DH gene, JH gene and CDR3 and found that the lengths of the DH gene were mainly distributed in 4–19 bp and up to 31 bp,

the lengths of the JH gene were mainly distributed in 3–15 bp and up to 23 bp, and the lengths of the CDR3 were mainly distributed in 18–54 bp (Figure S1D-F).

We further analyzed the length distribution and amino acid composition of Silver-black fox CDR3H, revealing a high degree of similarity in amino acid usage between Silver-black fox and Ussuri raccoon CDR3H (unpublished data from our laboratory). Both Silver-black fox and Ussuri raccoon belong to the Canidae family, and their CDR3H exhibit highly similar amino acid compositions, suggesting potential convergent evolution in certain immune system features possibly stemming from a shared ancestor. It is noteworthy that the cysteine (Cys) content in Silver-black fox CDR3H is extremely low, approximately 1% (Fig. 3). Additionally, we examined the length distribution curves of CDR3H for each

Silver-black fox sample (Figure S4A), along with changes in amino acid type composition and Shannon entropy values, revealing consistent patterns across all three samples (Figure S5A-C).

Analysis of SHM in the silver-black Fox IgH (FR1-FR3)

Since the germline sequences have high nucleotide similarity in the same family, we therefore analyzed the mapping of mutation distribution in the FR1-FR3 region of the VH1, VH3, VH9, and VH19 genes, as shown in Fig. 4A-D. As we already know, the mutations in all V genes are mainly concentrated in the CDR region (CDR1 and CDR2), in addition to that, there were some high-frequency mutation regions at the end of the FR3 region, such as VH1 and VH3, and there were a few positions in the FR1 region with high-frequency mutations, such as VH19, which indicates that SHM could occur at a higher frequency outside of the high mutation regions. Next, we counted the mutation types of SHM and found that the mutation types of all samples were concentrated in G > A and A > G (Fig. 4E-H).

Structure of the genomic organization and phylogenetic analysis of silver-black Fox Igκ

Consistent with the IgH method, we searched the Silver-black fox genome for the Vκ and Jκ genes of Igκ. The results showed that Silver-black fox Vκ genes were located on 5 scaffolds (Fig. 5A). We identified a total of 17 Vκ genes, of which 9 were potentially functional and 8 pseudogenes. We also identified 6 Jκ genes, 2 of which were potentially functional J genes, and they all possessed FGXG conserved structures (Fig. 5B). In addition, we identified one Cκ gene with a full length of approximately 320 bp (Fig. 5A). Immediately after that, we analyzed the Vκ genes into families based on nucleotide identity and found that the Vκ genes could be divided into three families (Fig. 5C). And the analysis revealed that the Vκ of the Silver-black fox was more closely related to the dog, followed by other mammals (Fig. 5D).

Analysis of the use of silver-black Fox Vκ and Jκ gene

The use of Vκ and Jκ is shown in Fig. 6, which is basically the similar for the three samples. Specifically, the use of IGKV2 was dominant (> 99%), and the use of other types of V genes was minimal (Fig. 6A). Regarding the Jκ genes

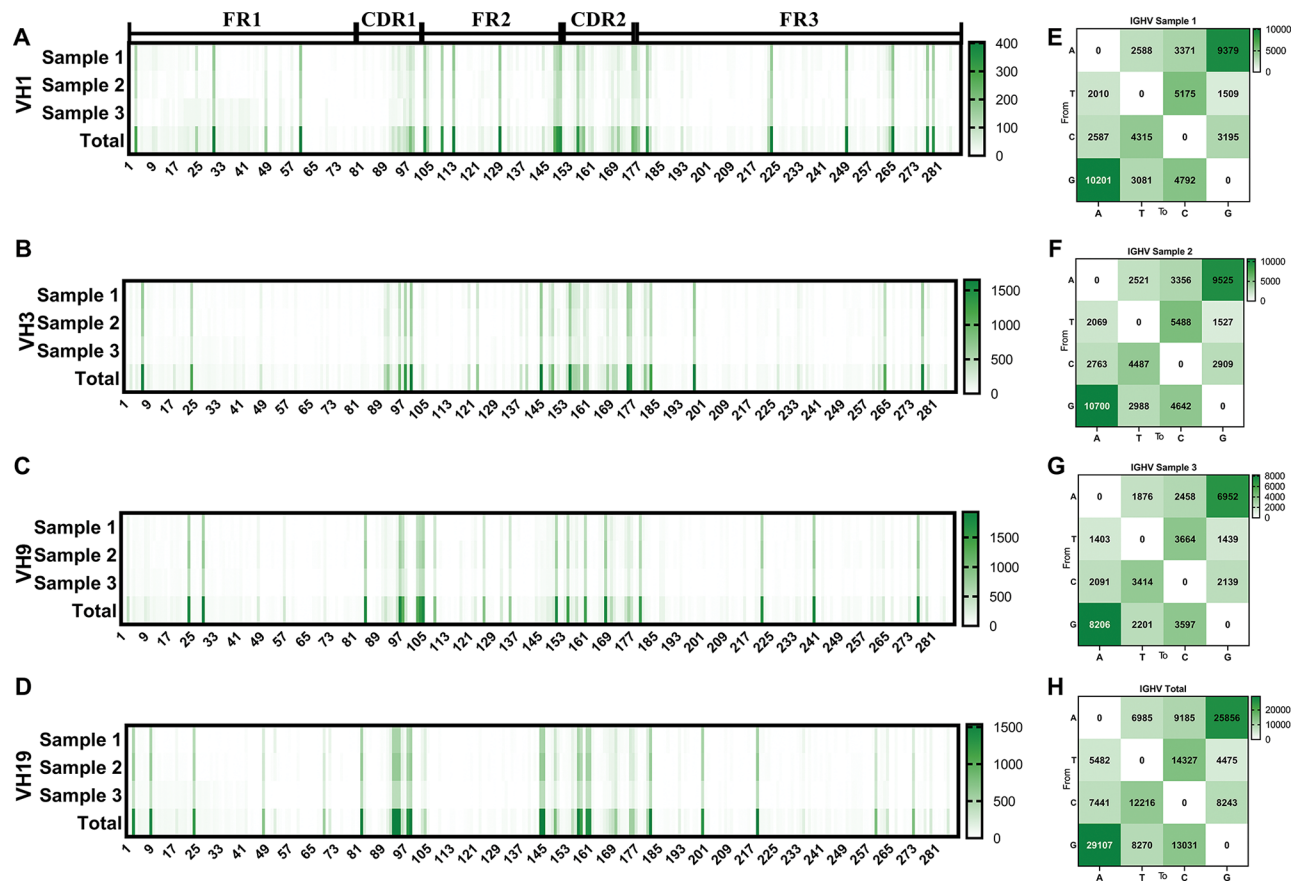


Fig. 4 The somatic hypermutation (SHM) of Silver-black Fox IgH. **A-D**: The distribution of SHM in Silver-black Fox IgH; **E-H**: The base mutation types of SHM in Silver-black Fox IgH

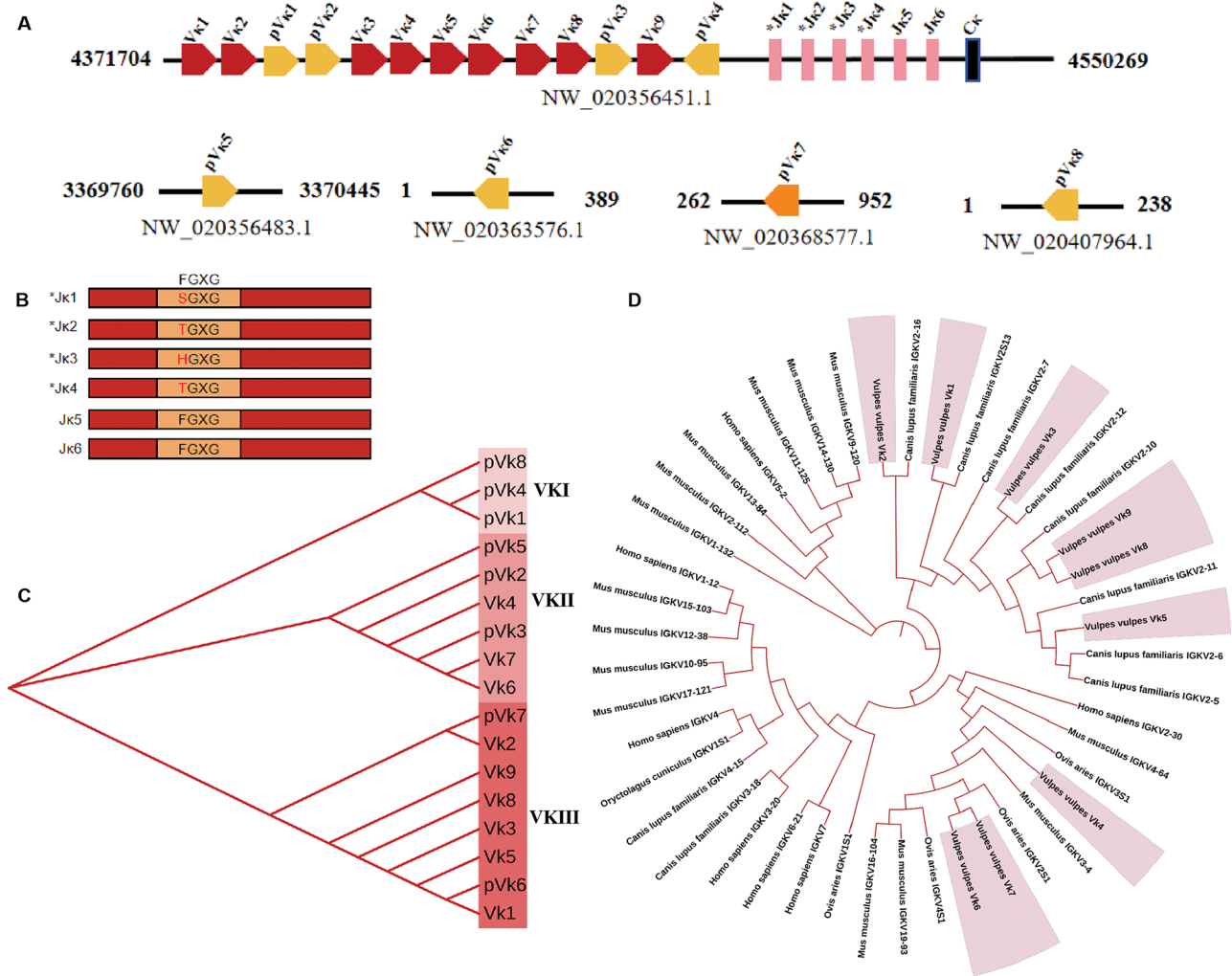


Fig. 5 Structure of the Genomic Organization and Phylogenetic Analysis of Silver-black Fox Igk. **A:** Schematic structure of the genomic organization of Silver-black Fox Igk; **B:** The structural variation of Silver-black Fox Jk; **C:** The phylogenetic tree of Silver-black Fox Vk; **D:** The phylogenetic tree of Vk in Silver-black Fox and representative vertebrate species. Note: Fig. 5A: The 5 scaffolds of the Igk gene are labeled with their corresponding ID sequence numbers. The start and end positions of each scaffold are labeled in the figure. Red arrows represent functional Vk genes, yellow arrows represent pseudogenes, and the head of each arrow indicates the orientation of the gene in the genome. Figure 5B: shows the conserved amino acid structure of Jk

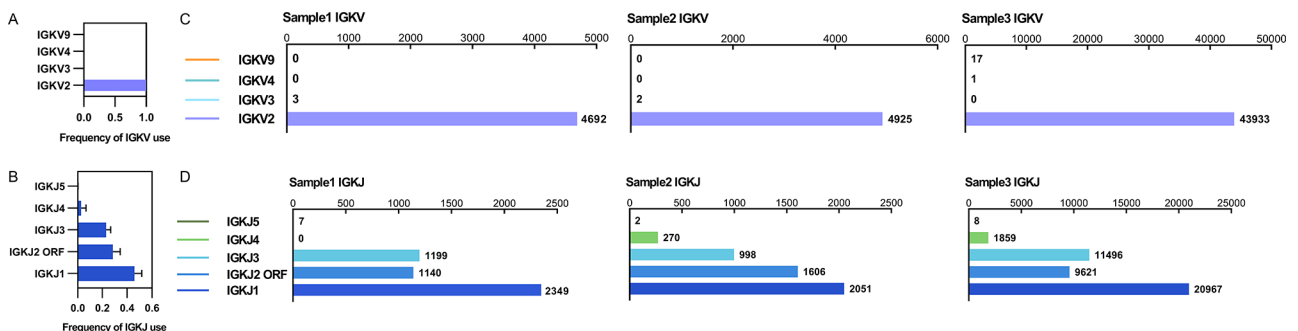


Fig. 6 Analysis of Silver-black Fox Vk, and Jk usage. **A&C:** Expression of the Silver-black Fox Vk; **B&D:** Expression of the Silver-black Fox Jk. Note: The X-axis numbers in Figure C-D represent read readings

expression, the use of IgκJ1 was dominant, utilization rate in the three samples were 50.03%, 41.6%, and 47.47% (Fig. 6B). In terms of the number of VJ genes used, the three samples showed a consistent trend in expression after recombination (Fig. 6C-D).

Analysis of V(D)J recombination diversity and junction diversity in the silver-black Fox Igκ

As shown in Figure S2A, we analyzed the recombination of Silver-black fox Vκ-Jκ. The expression of the three samples were basically consistent, the most expressed combinations were IGKV2-IGKJ1 and IGKV2-IGKJ3, and the expression share of these two combinations was more than 91.9% in all three samples, including 99.8% in sample 1. Subsequently, we found that random deletions of Vκ and Jκ genes were mainly distributed in 0–3 bp, where deletions of 0 bp and 3 bp do not affect post-recombination translation, suggesting that random deletions of Vκ and Jκ genes contribute relatively little to the diversity of Ig expression but affect the length of CDR3 (Figure S2B-C). N/P nucleotide insertions were mainly distributed at 0 bp, indicating that CDR3 length diversity was not related to the insertion of N/P nucleotides (Figure S2E-G). In addition, the length of Jκ gene was mainly distributed at 5–11 bp (Figure S2D), and the length of CDR3κ was mainly distributed at 24–30 bp (Figure S2H).

Analysis of the amino acid composition of Silver-black fox CDR3κ revealed that it was almost identical to raccoon CDR3κ as in previous findings, with only aromatic amino acids significantly higher than those of raccoon dog (unpublished data), which may be conducive to the further enrichment of the Silver-black fox antibody repertoire (Fig. 7). Further, we analyzed the length distribution curves of CDR3κ for each sample of Silver-black fox (Figure S4C), as well as the change in amino acid type composition and Shannon entropy values, and found that the three samples behaved consistently (Figure S5G-I).

Analysis of SHM in the silver-black Fox Igκ (FR1-FR3)

After comparison with the germline gene, we analyzed the SHM mutation distribution pattern of Vκ in a manner consistent with the SHM analysis of IgH. In addition to the CDR region with high-frequency mutation regions, there were a small number of high-frequency mutation regions in front of FR1 as well as at the end of FR3 (Fig. 8A-E). Immediately following this, we analyzed the SHM mutation types in Silver-black fox Igκ. As shown in Fig. 8F-I, the mutation types in all samples were clustered in G > A, C > T, T > C and A > G.

Structure of the genomic organization and phylogenetic analysis of silver-black Fox Igλ

As shown in Fig. 9A, the Silver-black fox Vλ was distributed on 9 scaffolds, and a total of 21 Vλ genes were identified, of which 17 were potentially functional. We also identified 11 Jλ genes, all with “FGXG” conserved sequence, which were located on a single scaffold in a Jλ-Cλ-Jλ-Cλ sequence with 8 Cλs (Fig. 9A-B). Subsequently, we found that the Vλ of the Silver-black fox could be classified into three families (Fig. 9C), and was more closely related to the Vλ gene in dog, followed by other mammals.

Analysis of the use of silver-black Fox Vλ and Jλ gene

In order to know the proportion of Vλ and Jλ genes used in the recombinantly expressed Igλ of Silver-black fox, we first classified the reads obtained from sequencing into IMGT-subgroups, and then analyzed the use of each type of gene. Specifically, IGLV1 was used in the largest proportion (> 55%), and regarding Jλ gene use, the most expressed genes were IGLJ6 (> 24%) and IGLJ4 (> 18%) (Fig. 10A&B). In terms of the number of VJ genes used, the trend of Vλ and Jλ gene use was consistent (Fig. 10C&D).

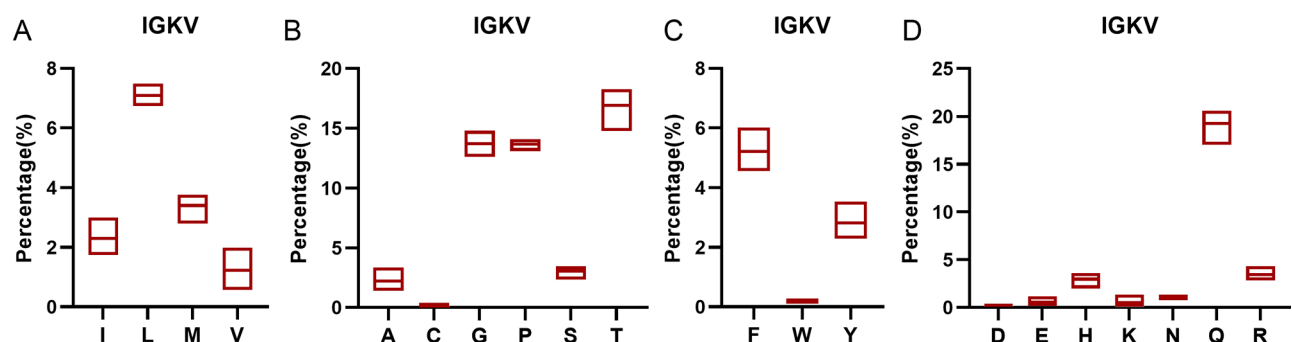


Fig. 7 Frequency of various amino acids used in CDR3κ of Silver-black Fox. **A:** Frequency of hydrophobic amino acids in CDR3κ of Silver-black Fox; **B:** Frequency of small molecular functional group amino acids in CDR3κ of Silver-black Fox; **C:** Frequency of use of aromatic amino acids in CDR3κ of Silver-black Fox; **D:** Frequency of use of charged amino acids in CDR3κ of Silver-black Fox

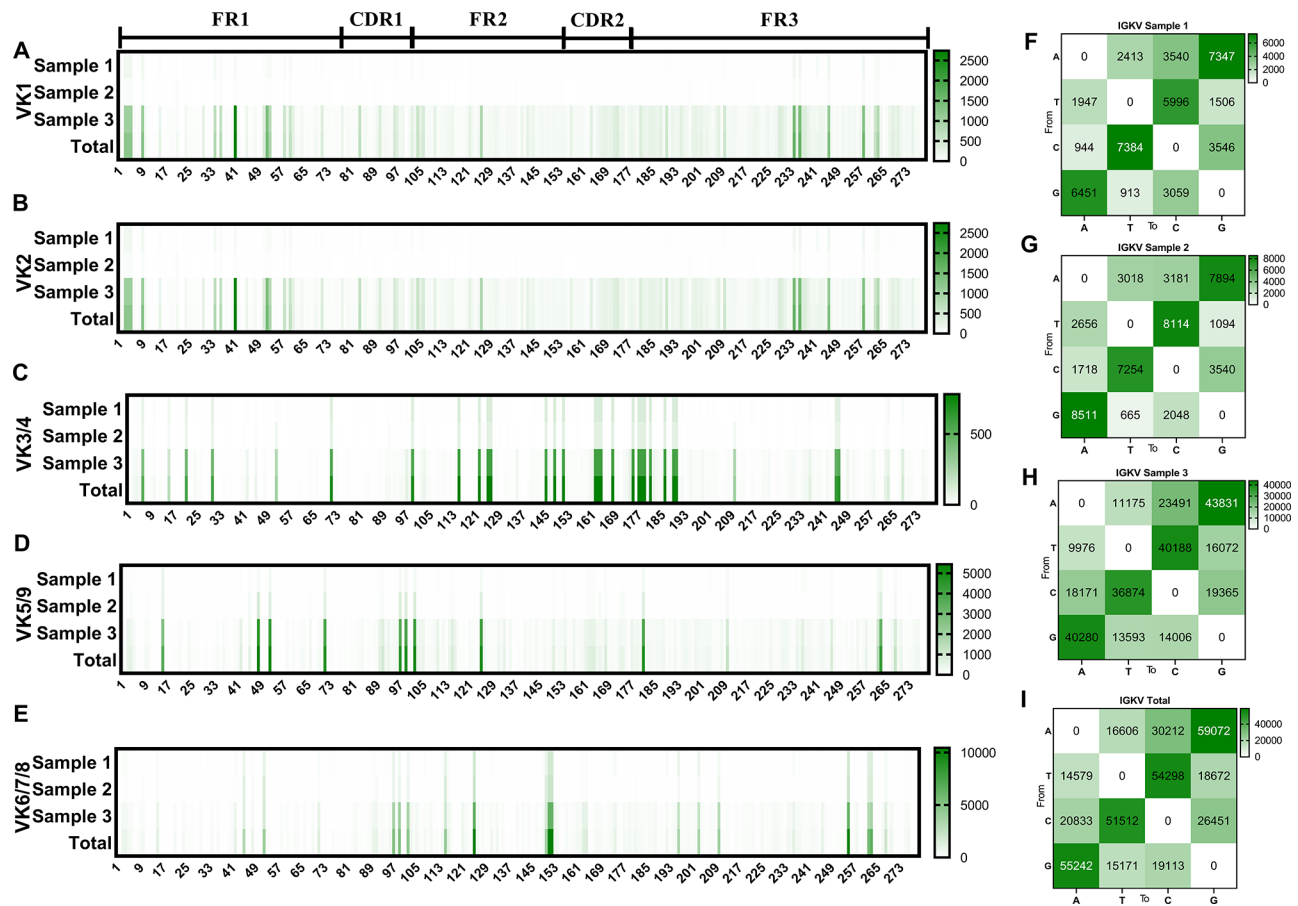


Fig. 8 The somatic hypermutation (SHM) of Silver-black Fox Igk. **A-E**: The distribution of SHM in Silver-black Fox Igk; **F-I**: The base mutation types of SHM in Silver-black Fox Igk

Analysis of V(D)J recombination diversity and junction diversity in the silver-black Fox Igλ

Similarly, we analyzed the VJ recombination of Igλ and showed that the more used combinations in sample 1 were IGLV1-IGLJ4 (22.0%), IGLV1-IGLJ6 (19.7%), the more used combinations in sample 2 were IGLV1-IGLJ4 (19.0%), IGLV1-IGLJ6 (18.9%), and in sample 3 the more used combinations were IGLV1-IGLJ6 (19.7%), IGLV1-IGLJ4 (13.8%), and all three samples had essentially the same expression (Figure S3A). Subsequently, we analyzed the length diversity distribution of CDR3λ. As shown in Figure S3B-C, random deletions of the V gene were mainly distributed in 0–7 bp and up to 31 bp in length, indicating that random deletions of the V gene had a greater impact on the length of CDR3 (Figure S3B). Random deletions of the Jλ gene were mainly distributed in 0–3 bp (Figure S3C). The insertion of the N/P nucleotide, which was mainly distributed in 0 bp, indicated that the insertion of the N/P nucleotide contributed to the length of CDR diversity contributed less (Figure S3E-G). Finally, we found that the length of Jλ gene was mainly distributed in 6–10 bp (Figure S3D) and the length of CDR3 was mainly distributed in 27–33 bp (Figure S3H).

Analysis of the amino acid composition of Silver-black fox CDR3λ revealed that it was almost identical to Silver-black fox CDR3κ, with a lower frequency of Cys and a relatively high frequency of aromatic amino acid usage (Fig. 11). Further, we analyzed the length distribution curves of Silver-black fox CDR3λ for each sample (Figure S4B), as well as the changes in amino acid type composition and Shannon entropy values, and found that the three individuals behaved consistently (Figure S5D-F).

Analysis of SHM in the silver-black Fox Igλ (FR1-FR3)

The distribution of SHM mutations in the FR1-FR3 region of the Vλ gene was analyzed, and as shown in Fig. 12A-D, the high-frequency mutation regions were mainly concentrated in the CDR region, and in the FR1 region, higher mutation frequency also appeared, which was similar to the results of IgH and Igκ. Subsequently, we counted the major mutation types in SHM and found that the mutation types in all samples were concentrated in G > A, C > T, T > C and A > G, with G > A and A > G predominating (Fig. 12E-H).

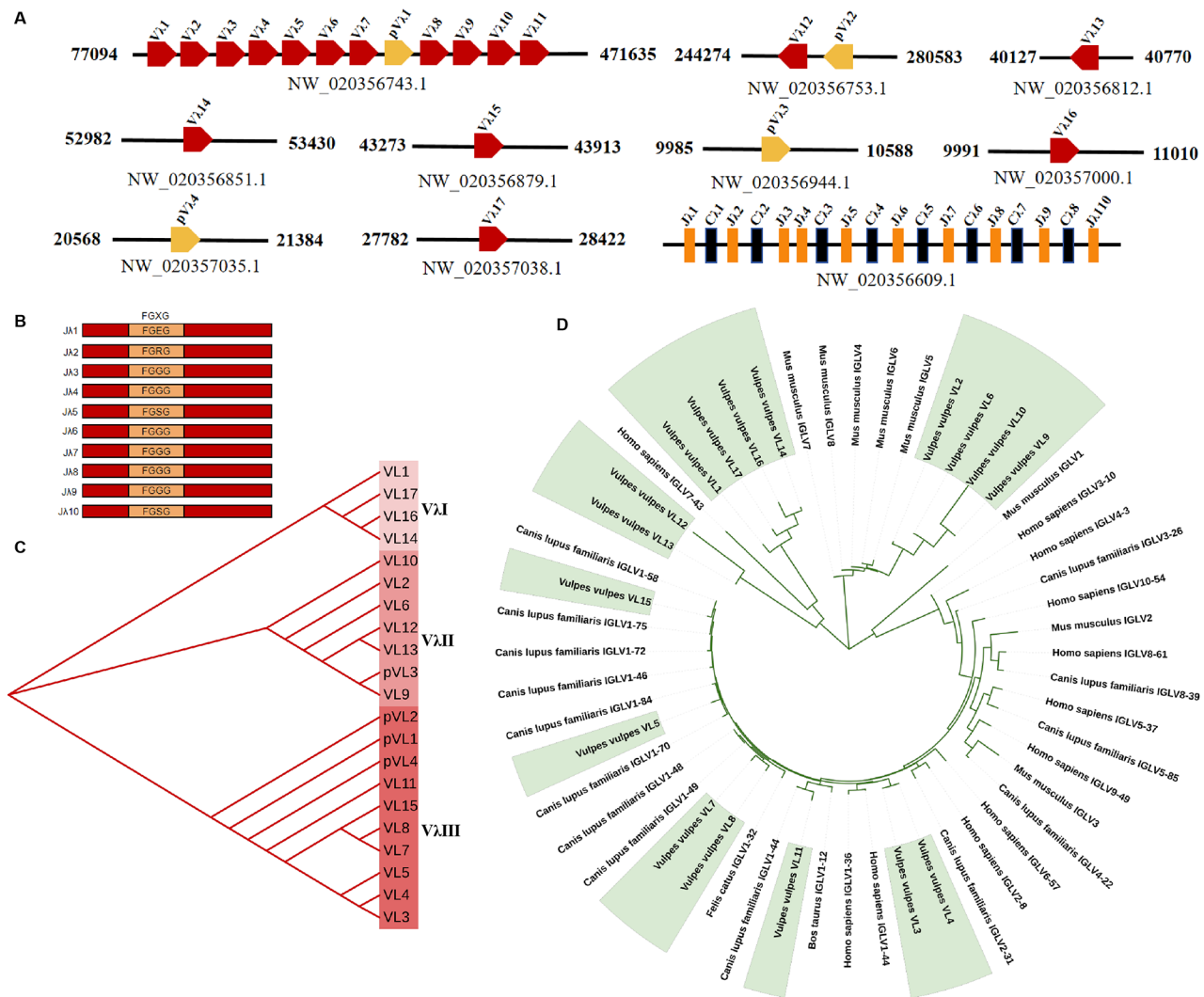


Fig. 9 Structure of the Genomic Organization and Phylogenetic Analysis of Silver-black Fox Igl. **A:** Schematic structure of the genomic organization of Silver-black Fox Igl; **B:** The structural variation of Silver-black Fox Jλ; **C:** The phylogenetic tree of Silver-black Fox Vλ; **D:** The phylogenetic tree of Vλ in Silver-black Fox and representative vertebrate species. Note: Fig. 9A: The 10 scaffolds of the Igl gene are labeled with their corresponding ID sequence numbers. The start and end positions of each scaffold are labeled in the figure. Red arrows represent functional Vλ genes, yellow arrows represent pseudogenes, and the head of each arrow indicates the orientation of the gene in the genome. Figure 9B: shows the conserved amino acid structure of Jλ

Discussion

In this study, we firstly identified the V genes, D genes, J genes and constant region genes that conform to the IMGT rules by a comparative genomics method using the published Silver-black fox genome [43], and constructed the Silver-black fox Ig gene loci maps (Figs. 1A and 5A, and Fig. 9A). Among them, the number of potentially functional VH genes was 32, Vκ genes was 9, Vλ genes was 17, DH genes was 9, JH genes was 3, Jκ genes was 6, and Jλ genes was 11, all located on different scaffolds of the genome. It is important to note that the number of germline genes identified in this study may be fewer than the actual number. This assumption is based on the observation that all germline genes retrieved in this study were classified under the IGLV1 subgroup. However, our

sequencing data revealed the expression of genes from the IGLV2, IGLV3, IGLV5, and IGLV8 subgroups. We attribute this discrepancy to the fact that the assembly level of the Silver-black fox genome (GCF_003160815.1) is at the scaffold level, which likely resulted in numerous genomic fragments remaining unassembled. As a result, the exploration of potential functional genes may have been insufficient. Additionally, the IgH loci in the Silver-black fox exhibit an inverse complementary arrangement, which may be due to the reversed placement of genomic scaffolds. In the Igκ, the Jλ and Cλ segments exist in clusters, an arrangement that is similarly expressed in mink, arctic fox, goats, horses and yaks [34, 36, 37, 44–46].

Furthermore, the domestic dog and the Silver-black fox both belong to the class Mammalia, order Carnivora,

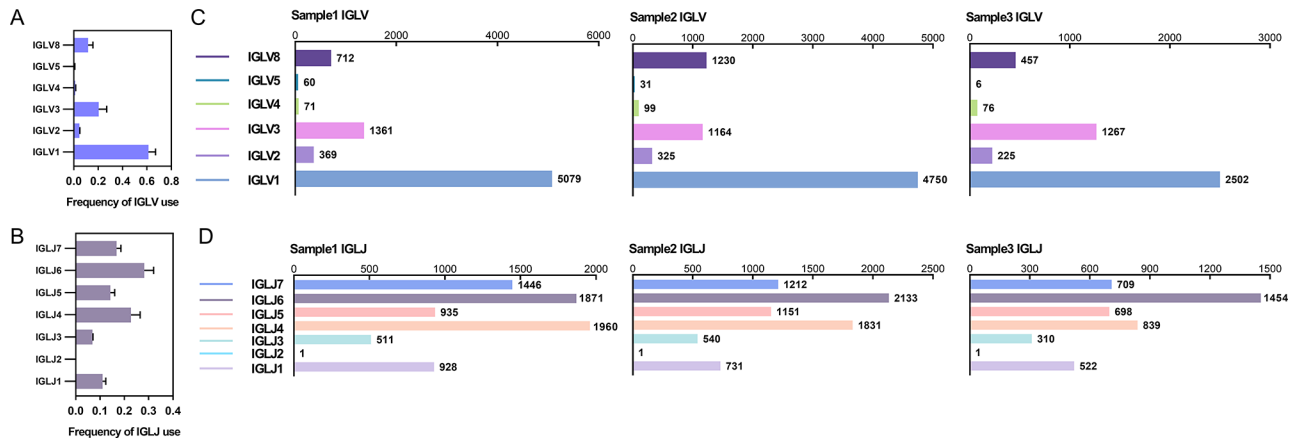


Fig. 10 Analysis of Silver-black Fox $V\lambda$, and $J\lambda$ usage. **A&C:** Expression of the Silver-black Fox $V\lambda$; **B&D:** Expression of the Silver-black Fox $J\lambda$. Note: The X-axis numbers in Figure C-D represent read readings

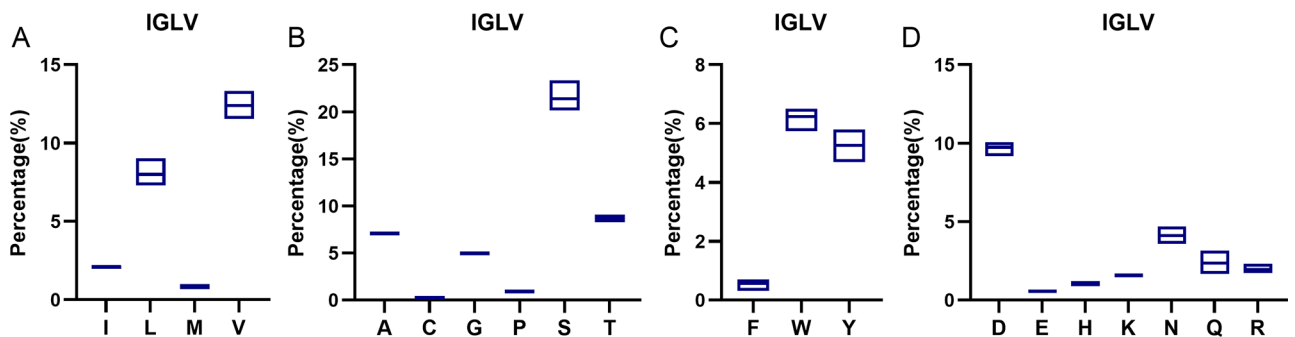


Fig. 11 Frequency of various amino acids used in CDR3 λ of Silver-black Fox. **A:** Frequency of hydrophobic amino acids in CDR3 λ of Silver-black Fox; **B:** Frequency of small molecular functional group amino acids in CDR3 λ of Silver-black Fox; **C:** Frequency of use of aromatic amino acids in CDR3 λ of Silver-black Fox; **D:** Frequency of use of charged amino acids in CDR3 λ of Silver-black Fox

and family Canidae, but they are classified under different genera, *Canis* and *Vulpes*, respectively. Despite the significant taxonomic differences at the genus level, phylogenetic studies indicate that the Ig genes of the two species share specific phylogenetic relatedness in their evolutionary context. Notably, a portion of the VH genes in the Silver-black fox, along with the majority of $V\lambda$ and $V\kappa$ genes, exhibit a high degree of clustering with those of the dog. This molecular evidence suggests a potential common evolutionary foundation for the Ig gene structures between the Silver-black fox and other canid species. However, most of the V genes in the Silver-black fox do not cluster with those of humans on the phylogenetic tree, indicating a significant divergence in the evolution of the immune system between the Silver-black fox and humans. Furthermore, some of the VH genes in the Silver-black fox form a distinct cluster, separate from that of the dog, thus reflecting systematic differences in the evolutionary dynamics of Ig genes between the dog and the Silver-black fox [14].

Immunocomplexes captured by NGS can give us more insight into B-cell immunogenetics and the abundance of recombinant post-antibody expression [47].

Regarding the ways in which Silver-black fox Ig diversity is expressed, our results suggest that VDJ recombination and SHM are the two most dominant mechanisms. GCV is typically observed in animals with a relatively simple subgroup classification of potentially functional V genes, serving to enhance the diversity of Ig expression. This mechanism has been reported in species such as chickens [48], Beijing ducks [49], and rabbits [50], among others.

In addition, the length of CDR3 provides more possibilities for its diverse expression. Specifically, when V(D)J is recombined, Silver-black fox IgH, Ig λ , and Ig κ show significant selective preferences for the V gene, the J gene, and similarly, IgH for the DH gene. This enriches the types of V(D)J recombination, one of the important components of Ig diversity. It is well known that the random deletion of V and J genes and the insertion of N and P nucleotides are important factors constituting the diversity of the length of the CDR3, which determines the richness of the type of protein conformation it expresses. Based on this, we analyzed the lengths of random deletion fragments at the 3' end of the V gene and at the 5' end of the J gene, as well as the lengths of random insertions of N and P nucleotides [51]. The contribution of the

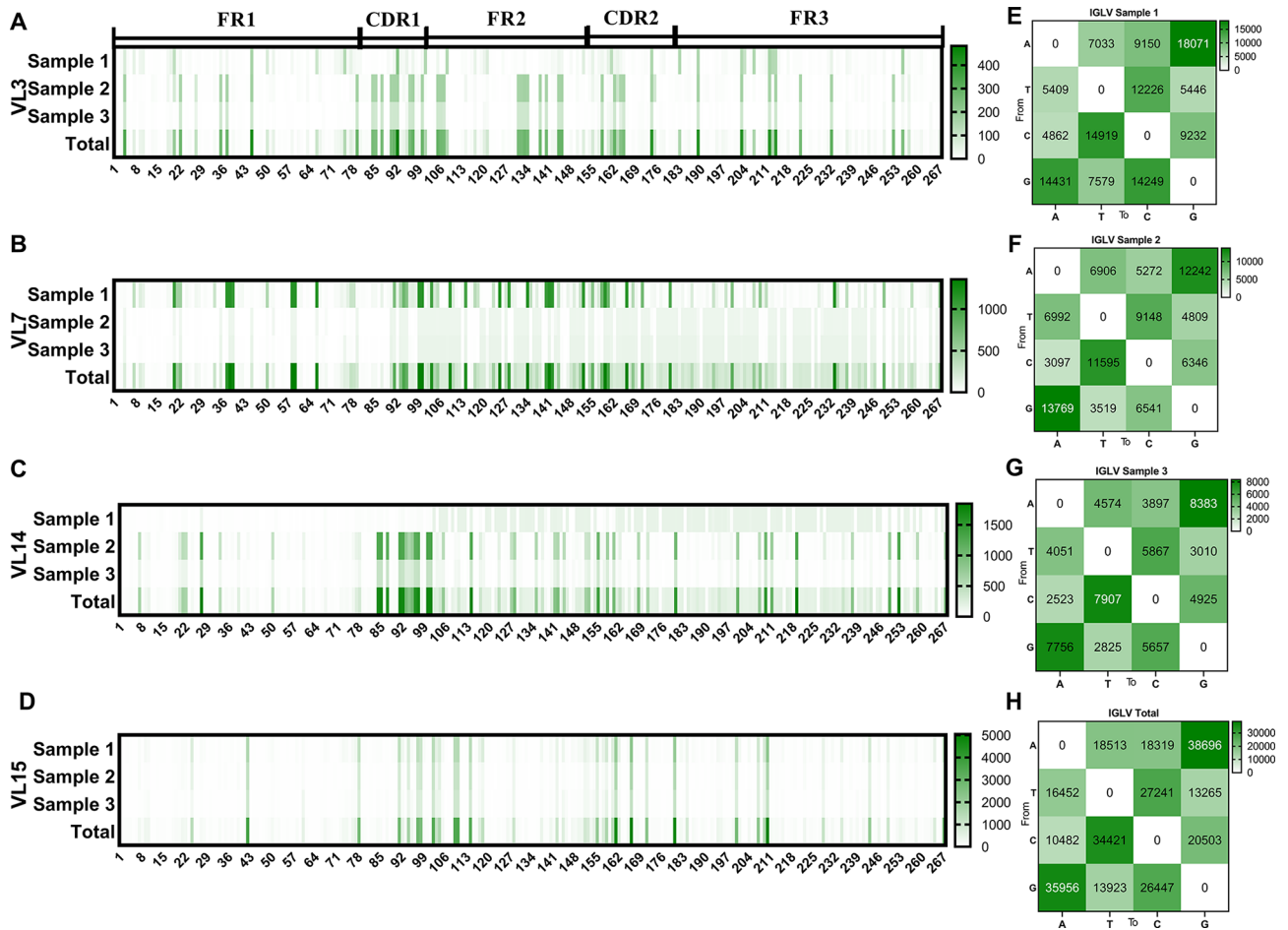


Fig. 12 The somatic hypermutation (SHM) of Silver-black Fox Igλ. **A-D**: The distribution of SHM in Silver-black Fox Igλ; **E-H**: The base mutation types of SHM in Silver-black Fox Igλ

3’VH to the length of the CDR3H in Silver-black foxes was comparable to that of human (6.5 ± 1.7 bp), mouse (5.8 ± 1.7 bp) and domestic cattle (8.8 ± 3.7 bp) [38, 52, 53]. It has been confirmed that bovine antibody repertoires are characterized by unusually long CDR3H, which form elaborate “knob-on-stalk” architectures rich in cysteine residues [54]. The pairing of Cys residues in different combinations forms disulfide bonds, which stabilize the structure of CDR3H and contribute to spatial diversity [55]. In contrast, in the Silver-black fox antibody repertoire, the frequency of Cys residues in CDR3H is only $0.7 \pm 0.3\%$, significantly lower than that in dogs [56]. The utilization of Cys in the light chain CDR3λ and CDR3κ is even lower, at $0.2 \pm 0\%$ and $0.1 \pm 0.2\%$, respectively. Studies have shown that, similar to human and mouse repertoires, the composition of dog CDR3H is predominantly characterized by tyrosine, serine, and glycine [56]. The amino acid composition of Silver-black fox CDR3H also exhibits these characteristics, suggesting that the Silver-black fox may rely on amino acid residues other than Cys to compensate for structural stability.

SHM is an important mechanism for the generation of antibody diversity after recombination of V(D) J, and amino acid changes induced by the mutation can increase the affinity of antibodies [15, 57, 58]. The mutation pattern of SHM in the IgH of the Silver-black fox is similar to that observed in yaks, domestic cattle, and mice, characterized by a high frequency of A-to-G and G-to-A mutations, suggesting that the mutation pattern of SHM is relatively conserved across species [38, 59]. Interestingly, our results showed that mutations in A and G were greater than mutations in T and C, this result was also verified in a recent study [58].

The study of Ig genes is not only a core component of immunological basic theory, but also an important bridge connecting basic research and clinical applications. Previous studies, based on the limited diversity of horse IgV, have successfully developed an efficient, rapid, and high-throughput monoclonal antibody screening platform [60]. As a fur-bearing animal, the Silver-black fox has long been threatened by viral diseases such as canine distemper virus (CDV) [61] and rabies virus (RV) [62].

Therefore, a deeper understanding of the selective usage and diversity characteristics of its IgV genes will not only help clarify its innate immune response mechanisms but also provide critical genetic resources for the development of specific antibodies, laying the foundation for the design of novel vaccines and immunotherapy strategies.

Conclusions

In conclusion, this study constructed a physical map of the Ig gene loci in the Silver-black fox genome and elucidated the factors contributing to the complexity of its expressed Igs repertoire using NGS. These findings enhance our understanding of Ig gene structure and expression diversity, complement immunological research on the Silver-black fox, and contribute to the conservation of its genetic resources and antibody development.

Abbreviations

AID	Activation-induced cytidine deaminase
BCR	B cell receptor
CDR	Complementarity determining region
CSR	Class switch recombination
DSB	Double strand break
DH/JH gene	Diversity/joining heavy gene
Jk/Jλ gene	Joining κ/λ gene
FR	Frame region
GCV	Gene conversion
IgH/L	Immunoglobulin heavy/light chain
Ig	Immunoglobulin
NGS	Next-generation sequencing
5'RACE	Rapid amplification of cDNA 5' ends
RAG	Recombination activating genes
RSS	Recombination signal sequences
SHM	Somatic hypermutation
TCR	T cell receptor
TdT	Terminal deoxynucleotidyl transferase
VH/Vκ/Vλ	Variable region heavy/κ/λ chain

Supplementary Information

The online version contains supplementary material available at <https://doi.org/10.1186/s12917-025-04676-1>.

Supplementary Material 1

Supplementary Material 2

Acknowledgements

We thank professor Chao Xu of the Jilin Agricultural University, for providing valuable samples for this experiment.

Author contributions

Xiaohua Yi: carried out the experiment and wrote the paper. Yanbo Qiu: data analysis and visualization. Puhang Xie: data curation; formal analysis; investigation. Shuhui wang and xiuzhu sun: edited the paper and funding. All authors approved the final version of the paper.

Funding

Project supported by "National Forage Industry Technology System Program (CARS-34)".

Data availability

Sequence data that support the findings of this study have been deposited in the NCBI (<https://www.ncbi.nlm.nih.gov/>), with the primary accession code PRJNA1079498.

Declarations

Ethics approval and consent to participate

All experimental procedures were conducted in compliance with the Regulations on the Administration of Laboratory Animal Affairs approved by the State Council of the People's Republic of China. The study received approval from the Institutional Animal Care and Use Committee of the Northwest A&F University. At the same time, informed consent was obtained from the animal owners for the use of all experimental animals.

Consent for publication

All authors have approved the manuscript and agree with its publication.

Competing interests

The authors declare no competing interests.

Received: 16 May 2024 / Accepted: 17 March 2025

Published online: 28 March 2025

References

- Kawasaki K, Ohta Y, Castro CD, Flajnik MF. The Immunoglobulin J chain is an evolutionarily co-opted chemokine. *Proc Natl Acad Sci U S A*. 2024;121(3):e2318995121.
- Gibson WS, Rodriguez OL, Shields K, Silver CA, Dorgham A, Emery M, Deikus G, Sebra R, Eichler EE, Bashir A, et al. Characterization of the Immunoglobulin lambda chain locus from diverse populations reveals extensive genetic variation. *Genes Immun*. 2023;24(1):21–31.
- Jin S, Sun Y, Liang X, Gu X, Ning J, Xu Y, Chen S, Pan L. Emerging new therapeutic antibody derivatives for cancer treatment. *Signal Transduct Target Ther*. 2022;7(1):39.
- Mikocziova I, Greiff V, Sollid LM. Immunoglobulin germline gene variation and its impact on human disease. *Genes Immun*. 2021;22(4):205–17.
- Gyorkei A, Johansen FE, Qiao SW. Systematic characterization of Immunoglobulin loci and deep sequencing of the expressed repertoire in the Atlantic Cod (*Gadus morhua*). *BMC Genomics*. 2024;25(1):663.
- Schmitz S, Soto C, Crowe JE, Meiler J. Human-likeness of antibody biologics determined by back-translation and comparison with large antibody variable gene repertoires. *MAbs*. 2020;12(1):1758291.
- Banach M, Harley ITW, Getahun A, Cambier JC. Comparative analysis of the repertoire of insulin-reactive B cells in type 1 diabetes-prone and resistant mice. *Front Immunol*. 2022;13:961209.
- Ott JA, Mitchell C, Sheppard M, Deiss TC, Horton JMC, Haakenson JK, Huang R, Kelley AR, Davis BW, Derr JN, et al. Evolution of Immunogenetic components encoding ultralong CDR H3. *Immunogenetics*. 2023;75(4):323–39.
- Sun Y, Huang T, Hammarström L, Zhao Y. The Immunoglobulins: new insights, implications, and applications. *Annu Rev Anim Biosci*. 2020;8:145–69.
- Liu H, May K. Disulfide bond structures of IgG molecules: structural variations, chemical modifications and possible impacts to stability and biological function. *MAbs*. 2012;4(1):17–23.
- Vidarsson G, Dekkers G, Rispen T. IgG subclasses and allotypes: from structure to effector functions. *Front Immunol*. 2014;5:520.
- Zhao Y, Pan-Hammarström Q, Kacsokovics I, Hammarström L. The Porcine Ig delta gene: unique chimeric splicing of the first constant region domain in its heavy chain transcripts. *J Immunol*. 2003;171(3):1312–8.
- Cui Z, Zhao H, Chen X. Molecular and functional characterization of two IgM subclasses in large yellow croaker (*Larimichthys crocea*). *Fish Shellfish Immunol*. 2023;134:108581.
- Pennell M, Rodriguez OL, Watson CT, Greiff V. The evolutionary and functional significance of germline Immunoglobulin gene variation. *Trends Immunol*. 2023;44(1).
- Chi X, Li Y, Qiu X. V(D)J recombination, somatic hypermutation and class switch recombination of Immunoglobulins: mechanism and regulation. *Immunology*. 2020;160(3):233–47.

16. Jeon BC, Kim YJ, Park AK, Song MR, Na KM, Lee J, An D, Park Y, Hwang H, Kim TD, et al. Dynamic O-GlcNAcylation governs long-range chromatin interactions in V(D)J recombination during early B-cell development. *Cell Mol Immunol.* 2025;22(1):68–82.
17. McGrath JJC, Park J, Troxell CA, Chervin JC, Li L, Kent JR, Changrob S, Fu Y, Huang M, Zheng NY, et al. Mutability and hypermutation antagonize immunoglobulin codon optimality. *Mol Cell.* 2025;85(2):430–e444436.
18. Di Noia JM, Neuberger MS. Molecular mechanisms of antibody somatic hypermutation. *Annu Rev Biochem.* 2007; 76.
19. Hozumi N, Tonegawa S. Evidence for somatic rearrangement of immunoglobulin genes coding for variable and constant regions. *Proc Natl Acad Sci U S A.* 1976;73(10):3628–32.
20. Kabat EA, Wu TT, Bilofsky H. Evidence supporting somatic assembly of the DNA segments (minigenes), coding for the framework, and complementarity-determining segments of immunoglobulin variable regions. *J Exp Med.* 1979;149(6):1299–313.
21. McCormack WT, Tjoelker LW, Thompson CB. Avian B-cell development: generation of an immunoglobulin repertoire by gene conversion. *Annu Rev Immunol.* 1991;9:219–41.
22. Schecter I, Burstein Y, Zemell R. Structure, organization, and controlled expression of the genes coding for the variable and constant regions of mouse immunoglobulin light chains. *Immunol Rev.* 1977; 36.
23. Gilfillan S, Dierich A, Lemeur M, Benoist C, Mathis D. Mice lacking TdT: mature animals with an immature lymphocyte repertoire. *Science.* 1993;261(5125):1175–8.
24. Sandor Z, Calicchio ML, Sargent RG, Roth DB, Wilson JH. Distinct requirements for Ku in N nucleotide addition at V(D)J- and non-V(D)J-generated double-strand breaks. *Nucleic Acids Res.* 2004;32(6):1866–73.
25. Bentolila LA, Olson S, Marshall A, Rougeon F, Paige CJ, Doyen N, Wu GE. Extensive junctional diversity in Ig light chain genes from early B cell progenitors of mu MT mice. *J Immunol.* 1999;162(4):2123–8.
26. Bogue M, Mossman H, Stauffer U, Benoist C, Mathis D. The level of N-region diversity in T cell receptors is not pre-ordained in the stem cell. *Eur J Immunol.* 1993;23(5):1185–8.
27. Golub R, André S, Hassanan A, Affaticati P, Larjani M, Fellah JS. Early expression of two TdT isoforms in the hematopoietic system of the Mexican Axolotl. Implications for the evolutionary origin of the N-nucleotide addition. *Immunogenetics.* 2004;56(3):204–13.
28. Jackson KJL, Gaeta B, Sewell W, Collins AM. Exonuclease activity and P nucleotide addition in the generation of the expressed immunoglobulin repertoire. *BMC Immunol.* 2004;5:19.
29. Ratcliffe MJH. Antibodies, immunoglobulin genes and the bursa of Fabricius in chicken B cell development. *Dev Comp Immunol.* 2006;30(1–2):101–18.
30. Kobayashi M, Wakaguri H, Shimizu M, Higasa K, Matsuda F, Honjo T. Ago2 and a miRNA reduce topoisomerase 1 for enhancing DNA cleavage in antibody diversification by activation-induced cytidine deaminase. *Proc Natl Acad Sci U S A.* 2023;120(18):e2216918120.
31. Briney B, Inderbitzin A, Joyce C, Burton DR. Commonality despite exceptional diversity in the baseline human antibody repertoire. *Nature.* 2019;566(7744):393–7.
32. Graf R, Seagal J, Otipoby KL, Lam K-P, Ayoub S, Zhang B, Sander S, Chu VT, Rajewsky K. BCR-dependent lineage plasticity in mature B cells. *Science.* 2019;363(6428):748–53.
33. Soto C, Bombardi RG, Branchizio A, Kose N, Matta P, Sevy AM, Sinkovits RS, Gilchuk P, Finn JA, Crowe JE. High frequency of shared clonotypes in human B cell receptor repertoires. *Nature.* 2019;566(7744):398–402.
34. Wu ML, Zhao HD, Tang XQ, Zhao WX, Yi XH, Li Q, Sun XZ. Organization and complexity of the Yak (*Bos Grunniens*) immunoglobulin loci. *Front Immunol.* 2022; 13.
35. Du L, Wang S, Zhu Y, Zhao H, Basit A, Yu X, Li Q, Sun X. Immunoglobulin heavy chain variable region analysis in dairy goats. *Immunobiology.* 2018;223(11):599–607.
36. Yu X, Du L, Wu M, Wu J, He S, Yuan T, Sun X. The analysis of organization and diversity mechanism in goat immunoglobulin light chain gene loci. *Immunobiology.* 2020;225(2):151889.
37. Sun Y, Wang C, Wang Y, Zhang T, Ren L, Hu X, Zhang R, Meng Q, Guo Y, Fei J, et al. A comprehensive analysis of germline and expressed immunoglobulin repertoire in the horse. *Dev Comp Immunol.* 2010;34(9):1009–20.
38. Ma L, Qin T, Chu D, Cheng X, Wang J, Wang X, Wang P, Han H, Ren L, Aitken R, et al. Internal duplications of DH, JH, and C region genes create an unusual IgH gene locus in cattle. *J Immunol.* 2016;196(10):4358–66.
39. Bao Y, Guo Y, Xiao S, Zhao Z. Molecular characterization of the VH repertoire in *Canis familiaris*. *Vet Immunol Immunopathol.* 2010;137(1–2):64–75.
40. Martin J, Pongstingl H, Lefranc M-P, Archer J, Sargan D, Bradley A. Comprehensive annotation and evolutionary insights into the canine (*Canis lupus familiaris*) antigen receptor loci. *Immunogenetics.* 2018;70(4):223–36.
41. Bao J. Analysis of fur color difference, cloning of pigment gene and TYRP1 function of red Fox and silver black Fox. Chinese Academy of Agricultural Sciences; 2015.
42. Lefranc M-P, Pommé C, Ruiz M, Giudicelli V, Foulquier E, Truong L, Thouvenin-Contet V, Lefranc G. IMGT unique numbering for immunoglobulin and T cell receptor variable domains and Ig superfamily V-like domains. *Dev Comp Immunol.* 2003;27(1):55–77.
43. Kukekova AV, Johnson JL, Xiang X, Feng S, Liu S, Rando HM, Kharlamova AV, Herbeck Y, Serdyukova NA, Xiong Z, et al. Red Fox genome assembly identifies genomic regions associated with tame and aggressive behaviours. *Nat Ecol Evol.* 2018;2(9):1479–91.
44. Yi X, Liu X, Sun X, Wang S. Structural profile and diversity of immunoglobulin genes in the Arctic Fox. *Vet J.* 2025;309:106295.
45. Yi X, Qiu Y, Wang S, Sun X. Analysis of immunoglobulin organization and complexity in Mink (*Neovison vison*). *Dev Comp Immunol.* 2024; 160.
46. Du LJ, Wang SH, Zhu YJ, Zhao HD, Basit A, Yu XH, Li QW, Sun XZ. Immunoglobulin heavy chain variable region analysis in dairy goats. *Immunobiology.* 2018;223(11):599–607.
47. Georgiou G, Ippolito GC, Beausang J, Busse CE, Wardemann H, Quake SR. The promise and challenge of high-throughput sequencing of the antibody repertoire. *Nat Biotechnol.* 2014;32(2):158–68.
48. Maizels N. Diversity achieved by diverse mechanisms: gene conversion in developing B cells of the chicken. *Cell.* 1987;48(3):359–60.
49. Guan X, Wang J, Ma L, Wang X, Cheng X, Han H, Zhao Y, Ren L. Multiple germline functional VL genes contribute to the IgL repertoire in ducks. *Dev Comp Immunol.* 2016;60:167–79.
50. Lavinder JJ, Hoi KH, Reddy ST, Wine Y, Georgiou G. Systematic characterization and comparative analysis of the rabbit immunoglobulin repertoire. *PLoS ONE.* 2014;9(6):e101322.
51. Fugmann SD, Lee AI, Shockett PE, Villey IJ, Schatz DG. The RAG proteins and V(D)J recombination: complexes, ends, and transposition. *Annu Rev Immunol.* 2000;18:495–527.
52. Koti M, Kataeva G, Kaushik AK. Organization of D(H)-gene locus is distinct in cattle. *Dev Biol (Basel).* 2008;132:307–13.
53. Koti M, Kataeva G, Kaushik AK. Novel atypical nucleotide insertions specifically at VH-DH junction generate exceptionally long CDR3H in cattle antibodies. *Mol Immunol.* 2010;47(11–12):2119–28.
54. Arras P, Zimmermann J, Lipinski B, Yanakieva D, Klewinghaus D, Krah S, Kolmar H, Pekar L, Zielonka S. Isolation of Antigen-Specific Unconventional Bovine Ultra-Long CDR3H Antibodies Using Cattle Immunization in Combination with Yeast Surface Display. *Methods In Molecular Biology (Clifton, NJ).* 2023;2681:113–129.
55. Wang F, Ekiert DC, Ahmad I, Yu W, Zhang Y, Bazirgan O, Torkamani A, Raudsepp T, Mwangi W, Criscitiello MF, et al. Reshaping antibody diversity. *Cell.* 2013;153(6):1379–93.
56. Steiniger SCJ, Dunkle WE, Bammert GF, Wilson TL, Krishnan A, Dunham SA, Ippolito GC, Bainbridge G. Fundamental characteristics of the expressed immunoglobulin VH and VL repertoire in different canine breeds in comparison with those of humans and mice. *Mol Immunol.* 2014;59(1):71–8.
57. Del Pozo-Yauner L, Herrera GA, Perez Carreon JI, Turbat-Herrera EA, Rodriguez-Alvarez FJ, Ruiz Zamora RA. Role of the mechanisms for antibody repertoire diversification in monoclonal light chain deposition disorders: when a friend becomes foe. *Front Immunol.* 2023;14:1203425.
58. Steele EJ, Franklin A, Lindley RA. Somatic mutation patterns at Ig and Non-Ig loci. *DNA Repair (Amst).* 2024;133:103607.
59. Wu M, Zhao H, Tang X, Zhao W, Yi X, Li Q, Sun X. Organization and complexity of the Yak (*Bos Grunniens*) immunoglobulin loci. *Front Immunol.* 2022;13:876509.
60. Wibmer CK, Mashilo P. Exploiting V-Gene bias for rapid, High-Throughput monoclonal antibody isolation from horses. *Viruses.* 2022; 14(10).

61. Prpić J, Lojkić I, Keros T, Krešić N, Jemeršić L. Canine distemper virus infection in the Free-Living wild canines, the red Fox (*Vulpes vulpes*) and Jackal (*Canis aureus moreoticus*), in Croatia. *Pathogens* 2023, 12(6).
62. Anderson RM, Jackson HC, May RM, Smith AM. Population dynamics of Fox rabies in Europe. *Nature*. 1981;289(5800):765–71.

Publisher's note

Springer Nature remains neutral with regard to jurisdictional claims in published maps and institutional affiliations.